Hindawi
Wireless Communications and Mobile Computing
Volume 2022, Article ID 9932652, 12 pages
https://doi.org/10.1155/2022/9932652

*Research Article*

# Splitting Energy of Transmit Power Serving Grouping Users in Full-Duplex Networks under Imperfect Hardware

**Nhan Duc Nguyen**,[1] **Anh-Tu Le**,[2] **and Dinh-Thuan Do**[3]

[1]*Faculty of Mechanical-Electrical and Computer Engineering, School of Engineering and Technology, Van Lang University, 69/68 Dang Thuy Tram Street, Ward 13, Binh Thanh District, 70000 Ho Chi Minh City, Vietnam*
[2]*Faculty of Electronics Technology, Industrial University of Ho Chi Minh City (IUH), Ho Chi Minh City 700000, Vietnam*
[3]*Electrical Engineering Department, University of Colorado Denver, Denver, CO 80204, USA*

Correspondence should be addressed to Anh-Tu Le; leanhtu@iuh.edu.vn

Received 25 August 2021; Revised 11 March 2022; Accepted 31 March 2022; Published 25 April 2022

Academic Editor: Abdul Basit



In this paper, we consider a wireless system providing power allocation fairness for grouping users by conducting a non-orthogonal multiple access (NOMA). In particular, a rigorous analysis is performed to evaluate performance of destination in a downlink of wireless system. With advances of NOMA, the user grouping scheme allows users to be shared the same frequency/power domain, and hence, fairness is guaranteed. In this regard, we focus on evaluation of the performance of a cell-center user and a cell-edge user in dedicated group. To enable forwarding function at cell-center user, we require the assistance of a full-duplex– (FD–) based relay to serve the cell-edge user. These users are assigned a fixed power allocation scheme. To characterize system performance, the closed-form expressions of the outage probability are computed for two users. To generalize channels in such system, Nakagami-*m* fading channels could be adopted to achieve complete theoretical analysis. Furthermore, we provide some comparisons of such FD NOMA under the impact of hardware impairment. We find that a significant improvement of outage probability can be achieved when the signal-to-noise ratio (SNR) at the source is high. Numerical results illustrate that both the analytical outage probability of the central user and the cell-edge user match the simulation results.

## 1. Introduction

Recent advances in wireless communications provide a new method to better serve the larger number of users [1, 2]. As one of these promising techniques, the non-orthogonal multiple access (NOMA) could be implemented in wireless system by employing non-orthogonal signal transmission at the transceiver [3–5]. On the transmit side, the users' information is superimposed in the power domain. The system relies on the way to enhance spectrum efficiency. In the NOMA system, multiple terminals can be served over the same resource block, thus employing that the NOMA is the effective way to enhance both spectrum efficiency and the sum rate. At the receiver side, successive interference cancellation (SIC) is conducted to decode the users' signal [6, 7]. Regarding SIC operation, by treating other signals as interference, the user with the best channel condition is given higher priority to decode. These advances of NOMA are prominent compared with orthogonal multiple access (OMA).

In the work of [6], an intermediate node acts as a relay to forward a signal from a source to a destination. The relaying system along with device-to-device is designed to achieve better transmission range or to enhance reliability by leveraging spatial diversity [7]. Higher spectrum efficiency can be obtained by enabling cognitive radio in NOMA systems [8]. More benefits are reported in the joint NOMA and cooperative communications, where NOMA users with poor channel conditions can be improved in their performance [9]. One or more dedicated relays are designed in relay-aided NOMA transmission to achieve performance improvement [10–17]. By considering arbitrary and optimal power allocation mode with full-duplex (FD) users operating

as decode-and-forward (DF) relays, the work in [9] studied the outage probability (OP) and ergodic sum-rate (ESR). In [13], NOMA-aided cooperative network is studied by exploring the model of Nakagami-$m$ channels. In this NOMA system, the closed-form expressions are derived to indicate the OP and the ergodic sum rate. In such a network, the source is required to serve simultaneously with multiple destinations through a relay using half duplex (HD). In similar studies [14–16], considering partial relay selection (PRS), a cooperative NOMA system with multiple relays can exhibit better performance in terms of and sum rate and OP. In [17], Nakagami-$m$ channels with a single FD-amplify and forward (AF) relay was studied to evaluate the outage performance and the ESR. In such a NOMA-based cooperative system, a fading-free self-interference link is adopted at the relay.

Recent works have considered the impact of hardware impairment and imperfect channel estimation in FD/HD cooperative NOMA-aided relaying systems. The works in [18–26] and references therein discussed the harmful impact of hardware impairment noise in various wireless technologies. The work of [18] especially focused on hardware impairment of FD/HD NOMA-aided relaying systems in Internet-of-things (IoT). In particular, the authors were concerned with the impact of hardware impairments via low-cost devices in practical IoT deployment. The authors derived exact OP and ergodic capacity expressions for near and far users under Rayleigh fading channels. In [19], the authors investigated the OP of a cooperative simultaneous wireless information and power transfer (SWIPT) NOMA-assisted multiple-relay network. The energy harvesting (EH) relays are also responsible for the communication between the base station and users. The EH relays operate under hardware impairment and imperfect channel state information (iCSI). PRS is exploited to select an EH relay to transmit information from the base station to a near and far user. Closed-form OP expressions are derived to understand deeply the impact of hardware impairments and iCSI.

Similarly, in [20], the authors examined the joint influence of residual hardware impairment (RHI) and iCSI on power beacon aided cooperative NOMA multiple-relay systems. By this way, the communication is enabled by the multiple relays harvesting energy from the power beacon. The communication from the base station to the far users is achieved only via the relays, while near users can receive information from either the base station or the relays or both. In addition, there is a direct link between the base station and far users. The authors derived exact OP expressions for the system users. Simulation results showed the existences of error floors in the OP performance curves attributed to RHIs and iCSI. In [21], the authors investigated the impact of hardware impairment and imperfect channel estimation in SWIPT NOMA-aided massive IoT systems. Communication between the base station and NOMA IoT devices is achieved via a direct link and the aid of multiple relays with EH and storage capability. PRS is utilized to select the optimal relay among the multiple relays to transmit information from the base station to the NOMA IoT devices. The authors also derived closed-form OP expressions and investigated the energy efficiency of the proposed system. In addition, the authors obtained the optimal power allocation strategy to maximize the sum rate in the high signal-to-noise ratio (SNR) region. Simulation results showed that hardware impairment harms performance and channel estimation is good for OP.

In [22], the authors examined how maximum-ratio transmission (MRT)/maximum-ratio combining (MRC) performs in NOMA-aided FD relay systems suffering from RHIs as well as imperfect CSI and imperfect SIC. The base station uses MRT and the multiple users utilize MRC, and the two-antenna relay relies on AF mode in its operation. The authors derived closed-form OP expressions under Nakagami-$m$ fading channels. The authors also obtained diversity and array gain tight lower bounds and asymptotic OP expressions. The simulation results demonstrated the necessity of loop-interference cancellation at the FD relay for the proposed system to outperform HD-NOMA systems. Moreover, the results proved that RHIs impact significant users with lower power coefficients but the diversity order is not affected. Also, imperfect CSI does not impact the system significantly.

*1.1. Related Works.* Considering the impact of hardware impairment, the authors in [23] investigated performance of all devices and self-interference at the FD relay on the detection performance of NOMA-assisted multiple-input multiple-output (MIMO) FD relaying system with MRT/MRC at the source and destination, respectively. The authors derived exact OP expressions, throughput, and symbol error rate (SER). Simulation results showed a significant impact of hardware impairment at high data rates on OP, throughput, and SER of the considered system when compared to the non-impaired version of the considered system. Furthermore, numerical results showed the introduction of error floors at the high SNR region of OP and SER performance curves. Fortunately, the introduction of MRT/MRC with more transmit antennas at the source than at the destination was found to enhance the OP and SER performance under hardware impairment conditions.

Moreover, in [24], the authors analyzed the performance of cooperative FD-NOMA relaying when in-phase and quadrature-phase imbalance (IQI) and imperfect SIC are considered. The authors derived exact OP and approximate analytical ESR expressions. Simulation results demonstrated that both NOMA-FD relaying and OMA-FD relaying are impacted in their OP and ESR performance in the moderate and high SNR region. However, OP of FD-NOMA relaying is impacted slightly than OMA-FD relaying. In addition, when FD-NOMA relaying is compared with the equivalent HD version, the far users of the FD-NOMA relaying suffer less from imperfect SIC. In [25], the authors considered the impact of hardware impairments on uplink FD-NOMA relaying in mobile edge computing (MEC) networks. The authors derived OP expressions of the proposed system. Numerical results showed the impact of hardware impairment on FD-NOMA relaying in MEC networks. In [26], the authors considered the impact of hardware impairment

on cooperative NOMA-FD system under Rician fading channels. The authors derived approximate analytical OP and ergodic rate expressions of the considered system. Numerical results highlight that NOMA-FD relaying enhances the ESR compared to the HD version of the proposed system.

*1.2. Our Contributions.* Motivated by the aforementioned papers, we deploy in this article an FD for performance improvement of two destinations in a NOMA-aided relay wireless system. Different from the aforementioned literature laid a solid foundation for the role of NOMA in Rayleigh fading to analyze system performance, the impact of FD-NOMA in general channel condition, namely, Nakagami-*m* fading, has not been well understood. Table 1 indicates some similar work. Based on the different parameter settings, the Nakagami-*m* fading channel can be reduce to how we analyze the system performance with multiple types of channel. Our main contribution is that the impact of hardware impairment is explored when we consider OP for the two destinations in our proposed system model. We also observe the benefits of the deployed relay in low transmit SNR regions in terms of optimal throughput performance at the cell edge user. Our paper provides several contributions compared with recent studies, shown in Table 1. Our contributions are listed as follows:

(i) We consider transmission in FD-NOMA system where a single antenna base station communicates with two devices arranged in a central and cell-edge positions. Communication between the base station and NOMA devices is achieved via a direct link between the cell-center device and the base station, while the single antenna FD relay with self-interference cancellation capability can forward signals to the cell-edge user. We study the outage and optimal throughput performance to determine the system performance under Nakagami-*m* fading channels and several practical hardware conditions

(ii) We then determine the signal-to-interference-plus-noise ratios (SINRs) of the two devices and use them to formulate exact OP and optimal throughput formulas. The derived expressions are validated by the Monte-Carlo simulations

(iii) We analyze and compare the OP and optimal throughput under various conditions. In particular, we find that hardware impairment, self-interference at the FD relay, the fixed rate, and the channel fading parameter are the main impacts on OP and optimal system throughput. The obtained numerical results demonstrate the impact of low-cost devices on OP and optimal throughput via many practical scenarios

*1.3. Organization.* The rest of this paper is organized as follows. Section 2 describes the downlink NOMA-aided FD relay system under Nakagami-*m* fading channels. In Section 3, we consider the scenario of NOMA in terms of outage performance. In Section 4, we consider optimal throughput performance. In Section 5, we provide extensive numerical simulations, and Section 6 concludes the paper.

## 2. System Model

We consider a cooperative Relay-aided NOMA system. In here, we assume a base station (S) and two destinations $D_1$ and $D_2$ with a help relay (R) in full-duple (FD) mode as in Figure 1. We consider $D_2$ as the central user, while the cell-edge user is $D_1$. In addition, all devices are equipped with a single antenna. We set $g_{SR}$ as the channel between S and R, $g_{SD_2}$ is the channel between S and $D_2$, $g_{RD_1}$ is the channel between R and $D_2$, and $g_R$ is the residual self-interference at R. Moreover, all the channels follows Nakagami-*m* channel fading. In addition, we consider the perfect CSI for all channels as [8].

The received signal from S to R is given by

$$y_R = \left(\sqrt{P_S\beta_2}x_2 + \sqrt{P_S\beta_1}x_1 + \varpi_{R,t}\right)g_{SR} + \varpi_{R,r} + \sqrt{P_R}\tau g_R x_1 + n_R, \tag{1}$$

where $P_S$ is the transmit power at S, $P_R$ is the transmit power at R, $\beta_1$ and $\beta_2$ are the power allocation coefficients, and $\varpi_{R,t}$ and $\varpi_{R,r}$ are the distortion noises with $CN(0, P_S\eta_{R,t}^2)$ and $CN(0, P_S|g_{SR}|^2\eta_{R,r}^2)$, respectively. $\eta_{R,t}^2$ and $\eta_{R,r}^2$ are the level of hardware impairments at S and R as in [27], $\tau(0 \le \tau \le 1)$ is the level of self-interference (SI), and $n_R$ denotes the additive white Gaussian noise (AWGN) with $CN(0, \sigma^2)$. When the signal $x_2$ is detected at R, the signal to-interference plus noise ratio (SINR) at R is expressed as

$$\begin{aligned}\Gamma_{R,x_1} &= \frac{P_S\beta_1|g_{SR}|^2}{P_S\beta_2|g_{SR}|^2 + P_S|g_{SR}|^2\left(\eta_{R,t}^2 + \eta_{R,r}^2\right) + P_R\tau|g_R|^2 + \sigma_{SR}^2} \\ &= \frac{\mu_S\beta_1|g_{SR}|^2}{\mu_S\beta_2|g_{SR}|^2 + \mu_S|g_{SR}|^2\left(\eta_{R,t}^2 + \eta_{R,r}^2\right) + \mu_R\tau|g_R|^2 + 1},\end{aligned} \tag{2}$$

where $\mu_S = P_S/\sigma^2$ and $\mu_R = P_R/\sigma^2$. Then, $R$ forwards the signal $x_1$ when detected successful. Therefore, the signal at $D_1$ is given by

$$y_{RD_1} = \left(\sqrt{P_R}x_1 + \varpi_{D_1,t}\right)g_{RD_1} + \varpi_{D_1,r} + n_{D_1}, \tag{3}$$

where $\varpi_{D_1,t}$ and $\varpi_{D_1,r}$ are the distortion noises with $CN(0, P_R\eta_{D_1,t}^2)$ and $CN(0, P_R|g_{RD_1}|^2\eta_{D_1,r}^2)$, respectively; $\eta_{D_1,t}^2$ and $\eta_{D_1,r}^2$ are the level of hardware impairments at $R$ and $D_1$; and $n_{D_1}$ is the AWGN. Then, the SINR when detecting $x_1$

Table 1: A comparison of existing works with our study on the impact of hardware impairment.

| Scheme | Reference | Major contributions |
|---|---|---|
| Half/full-duplex-NOMA-IoT | [18] | Hardware impairment of FD/HD NOMA-aided relaying systems is investigated. The exact OP and ergodic capacity expressions can be achieved for near and far users under Rayleigh fading channels |
| EH-SWIPT-NOMA | [19] | The OP performance is evaluated for a cooperative SWIPT NOMA-assisted multiple-relay network. This system employs EH relays to enhance transmission from the base station to users. The degraded performance is considered under joint impact of hardware impairment and iCSI |
| Power beacon-NOMA | [20] | The joint influences of RHIs and iCSI on power beacon aided cooperative NOMA multiple-relay systems are examined since the multiple relays harvesting energy are enabled |
| FD-NOMA | [23] | The impact of hardware impairment at all devices and self-interference at the FD relay is studied for NOMA-assisted MIMO FD relaying system |
| FD-NOMA-MEC | [25] | The impact of hardware impairments is studied at uplink NOMA-aided FD relaying in mobile edge computing (MEC) networks |
| FD-NOMA | Our work | We consider transmission assisted by NOMA where a single antenna base station communicates with two devices arranged in a central and cell-edge position. The evaluations of outage and throughput performance are provided under Nakagami-$m$ fading channels and several practical hardware conditions |

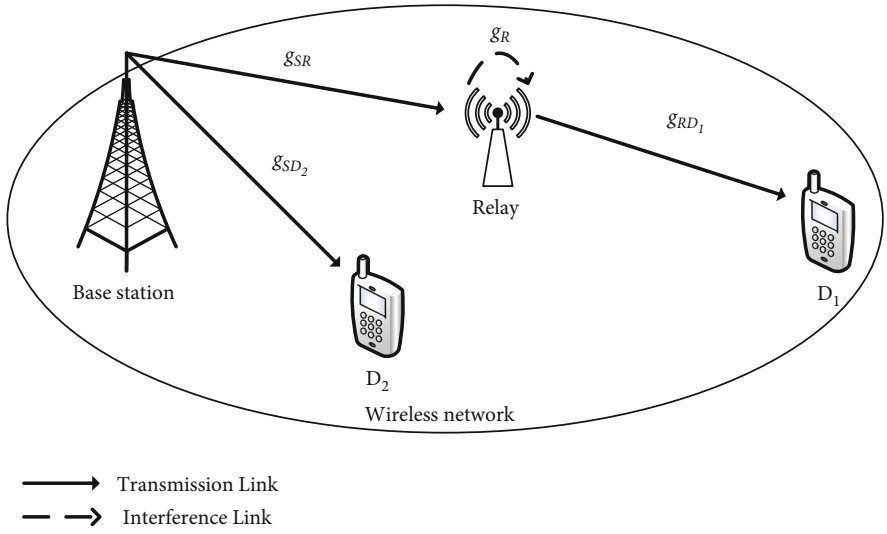


Figure 1: System model of NOMA relying on FD-assisted relay.

at $D_1$ is given by

$$\Gamma_{D_1,x_1} = \frac{P_R\left|g_{RD_1}\right|^2}{P_R\left|g_{RD_1}\right|^2\left(\eta_{D_1,t}^2+\eta_{D_1,r}^2\right)+\sigma^2} = \frac{\mu_R\left|g_{RD_1}\right|^2}{\mu_R\left|g_{RD_1}\right|^2\left(\eta_{D_1,t}^2+\eta_{D_1,r}^2\right)+1}. \tag{4}$$

Meanwhile, the received signal at $D_2$ can be expressed as

$$y_{SD_2} = \left(\sqrt{P_S\beta_1}x_1+\sqrt{P_S\beta_2}x_2+\omega_{D_2,t}\right)g_{SD_2}+\omega_{D_2,r}+n_{D_2}, \tag{5}$$

where $\omega_{D_2,t}$ and $\omega_{D_2,r}$ are the distortion noises with $CN(0, P_S\eta_{D_2,t}^2)$ and $CN(0, P_S|g_{RD_2}|^2\eta_{D_2,r}^2)$, respectively; $\eta_{D_2,t}$ and $\eta_{D_2,r}$ are the level of hardware impairments at S and $D_2$; and $n_{D_2}$ is the AWGN. Thus, the SINR when detecting the signal $x_1$ at $D_2$ is given by

$$\begin{aligned}\Gamma_{D_2,x_1} &= \frac{P_S\beta_1\left|g_{SD_2}\right|^2}{P_S\beta_2\left|g_{SD_2}\right|^2+P_S\left|g_{SD_2}\right|^2\left(\eta_{D_2,t}^2+\eta_{D_2,r}^2\right)+\sigma^2}\\ &= \frac{\mu_S\beta_1\left|g_{SD_2}\right|^2}{\mu_S\beta_2\left|g_{SD_2}\right|^2+\mu_S\left|g_{SD_2}\right|^2\left(\eta_{D_2,t}^2+\eta_{D_2,r}^2\right)+1}.\end{aligned} \tag{6}$$

Moreover, by applying SIC, the SINR at $D_2$ to detect its own signal $x_2$ is given by

$$\Gamma_{D_2,x_2} = \frac{\mu_S\beta_2\left|g_{SD_2}\right|^2}{\mu_S\left|g_{SD_2}\right|^2\left(\eta_{D_2,t}^2+\eta_{D_2,r}^2\right)+1}. \tag{7}$$

## 3. Outage Performance

In this section, we analyze the outage probability of two users $D_1$ and $D_2$. The channel of $g_k$ with $k \in SR, RD_1, SD_2, R$ is given as follows [8]:

$$f_{|g_k|^2}(\gamma) = \left(\frac{m_k}{\Omega_k}\right)^{m_k} \frac{\gamma^{m_k-1}}{\Gamma(m_k)} e^{-\frac{m_k}{\Omega_k}\gamma}, \tag{8}$$

where $m_k$ is the fading severity parameter and $\Omega_k$ being the average power.

*3.1. Outage Probability of $D_2$.* The outage probability of the system is written as follows [28]:

$$P_{\text{out}}^{D2} = 1 - \Pr\left(\Gamma_{D_2,x_1} > \vartheta_1, \Gamma_{D_2,x_2} > \vartheta_2\right), \tag{9}$$

where $\vartheta_1 = 2^{\nu_1} - 1$, $\vartheta_2 = 2^{\nu_2} - 1$, $\nu_1$, and $\nu_2$ denotes the target rate. With the help of (6) and (7), (9) is expressed as

$$P_{\text{out}}^{D2} = 1 - \Pr\left(\left|g_{SD_2}\right|^2 > \frac{\chi}{\mu_S}\right) = 1 - \int_{\frac{\chi}{\mu_S}}^{\infty} f_{\left|g_{SD_2}\right|^2}(\gamma) d\gamma, \tag{10}$$

where $\kappa_{D_2,1} = \beta_1 - \vartheta_1\beta_2 - \vartheta_1(\eta_{D_2,t}^2 + \eta_{D_2,r}^2)$, $\kappa_{D_2,2} = \beta_2 - \vartheta_2(\eta_{D_2,t}^2 + \eta_{D_2,r}^2)$, and $\chi = \max\left((\vartheta_1/\kappa_{D_1,1}), (\vartheta_2/\kappa_{D_1,2})\right)$. Using (8) and ([29], 3.351.2), the closed-form expression of $D_2$ is given by

$$\begin{aligned} P_{\text{out}}^{D2} &= 1 - \int_{\frac{\chi}{\mu_S}}^{\infty} \left(\frac{m_{SD_2}}{\Omega_{SD_2}}\right)^{m_{SD_2}} \frac{\gamma^{m_{SD_2}-1}}{\Gamma\left(m_{SD_2}\right)} e^{-\frac{m_{SD_2}}{\Omega_{SD_2}}\gamma} d\gamma \\ &= 1 - \sum_{a=0}^{m_{SD_2}-1} \frac{1}{a!} \left(\frac{m_{SD_2}\chi}{\Omega_{SD_2}\mu_S}\right)^a e^{-\frac{m_{SD_2}\chi}{\Omega_{SD_2}\mu_S}}. \end{aligned} \tag{11}$$

*3.2. Outage Probability of $D_1$.* As the main result reported in [28], the outage probability of $D_1$ is expressed as

$$P_{\text{out}}^{D1} = 1 - \Pr\left(\Gamma_{R,x_1} > \vartheta_1, \Gamma_{D_1,x_1} > \vartheta_1\right). \tag{12}$$

**Proposition 1.** *The closed-form expression of $D_1$ can be expressed as*

$$\begin{aligned} P_{\text{out}}^{D1} = 1 - &\sum_{b=0}^{m_{\text{SR}}-1} \sum_{c=0}^{b} \sum_{n=0}^{m_{RD_1}-1} \binom{b}{c} \frac{\Gamma(m_R + c)(\mu_R)^c e^{-m_{\text{SR}}\vartheta_1/\Omega_{\text{SR}}\mu_S\kappa_R - m_{RD_1}\vartheta_1/\Omega_{RD_1}\mu_R\kappa_{D_1}}}{\Gamma(m_R) b! n!} \left(\frac{m_R}{\Omega_R}\right)^{m_R} \\ &\times \left(\frac{m_{\text{SR}}\vartheta_1}{\Omega_{\text{SR}}\mu_S\kappa_R}\right)^b \left(\frac{m_R}{\Omega_R} + \frac{m_{\text{SR}}\vartheta_1\mu_R}{\Omega_{\text{SR}}\mu_S\kappa_R}\right)^{-m_R-c} \left(\frac{m_{RD_1}\vartheta_1}{\Omega_{RD_1}\mu_R\kappa_{D_1}}\right)^n. \end{aligned} \tag{13}$$

*Proof.* See the appendix. □

## 4. Asymptotic Outage Probability Analysis

In this section, we derive an asymptotic OP expression at high-SNR $\mu_S = \mu_R \longrightarrow \infty$. Then, we apply the first-order Maclaurin series expansions $e^{-x} \simeq 1 - x$. Thus, the asymptotic OP of $D_2$ can be expressed by

$$P_{\text{out}}^{D2,\infty} = 1 - \sum_{a=0}^{m_{SD_2}-1} \frac{1}{a!} \left(\frac{m_{SD_2}\chi}{\Omega_{SD_2}\mu_S}\right)^a \left(1 - \frac{m_{SD_2}\chi}{\Omega_{SD_2}\mu_S}\right). \tag{14}$$

Similarly, the asymptotic OP of $D_1$ is given by

$$\begin{aligned} P_{\text{out}}^{D1} = 1 - &\sum_{b=0}^{m_{\text{SR}}-1} \sum_{c=0}^{b} \sum_{n=0}^{m_{RD_1}-1} \binom{b}{c} \left(\frac{m_R}{\Omega_R}\right)^{m_R} \frac{\Gamma(m_R + c)(\mu_R)^c}{\Gamma(m_R) b! n!} \left(\frac{m_{RD_1}\vartheta_1}{\Omega_{RD_1}\mu_R\kappa_{D_1}}\right)^n \\ &\times \left(\frac{m_{\text{SR}}\vartheta_1}{\Omega_{\text{SR}}\mu_S\kappa_R}\right)^b \left(\frac{m_R}{\Omega_R} + \frac{m_{\text{SR}}\vartheta_1\mu_R}{\Omega_{\text{SR}}\mu_S\kappa_R}\right)^{-m_R-c} \left(1 - \frac{m_{\text{SR}}\vartheta_1}{\Omega_{\text{SR}}\mu_S\kappa_R} - \frac{m_{RD_1}\vartheta_1}{\Omega_{RD_1}\mu_R\kappa_{D_1}}\right). \end{aligned} \tag{15}$$

## 5. Optimal Throughput Analysis

In this section, we carry out the optimal analysis of the throughput performance. More particularly, we offer a method for determining the best value of $T_{\text{out},i}^*$, which results in the system's maximum throughput.

Based on achievable outage probability, throughput is the ability to transmit signals at fixed rate $\nu_i$. In particular, the throughput of each user is given by [8].

$$T_{\text{out},i} = \left(1 - P_{\text{out},i}^*\right)\nu_i. \tag{16}$$

The optimal points of such throughput as varying target rates of $\nu_i$ is expressed as

$$T_{\text{out},i}^* = \arg\max\left\{T_{\text{out},i}(\nu_i)\right\}. \tag{17}$$

Based on this algorithm, the optimal values of throughput can be obtained properly. We expect to verify such algorithm in next section.

**Input:** $P_{\text{out}}^{Di}$
**OutPut:** Optimal value $T_{\text{out},i*}^{*}$
1: Set $\nu_i^{\alpha} \longleftarrow [0 : 0.25 : 5]$ is used for the $X$-axis
2: Initialize $f \longleftarrow zeros(1, length(\nu_i^{\alpha}))$ and $T_{\text{out},i} \longleftarrow zeros(1, length(\nu_i^{\alpha}))$
3: **for** $k = 0$: $length(\nu_i^{\alpha})$ **do**
4: $\nu_i \longleftarrow \nu_i^{\alpha}(k)$
5: Compute $\phi_i(:,k) \longleftarrow P_{\text{out}}^{Di}(\nu_i)$
6: $T_{\text{out},i}(:,k) \longleftarrow [1-\phi_i(:,k)]\nu_i$
7: **end for**
8: $[\sim, i] \longleftarrow \arg\max [T_{\text{out},i}(:,;)]$
9: **Return** $T_{\text{out},i}^{*} \longleftarrow T_{\text{out},i}(:,i)$

Algorithm 1: The algorithm of finding the optimal throughput coefficient $T_{\text{out},i}^{*}$.

Table 2: Table of parameters.

| System parameters | Value |
|---|---|
| The power allocation | $\beta_1 = 0.7$ and $\beta_2 = 0.3$ |
| The level of self-interference | $\tau = 0.1$ |
| The target rate | $\nu_1 = 0.5$ and $\nu_2 = 1$ bit per channel use |
| The parameter of channel | $\Omega = \Omega_{SR} = \Omega_{RD_1} = \Omega_{SD_2} = \Omega_R = 1$ |
| The level of hardware impairments | $\eta_t^2 = \eta_{R,t}^2 = \eta_{D_1,t}^2 = \eta_{D_2,t}^2$ and $\eta_r^2 = \eta_{R,r}^2 = \eta_{D_1,r}^2 = \eta_{D_2,r}^2$ |
| The fading severity parameter | $m = m_{SR} = m_{RD_1} = m_{SD_2} = m_R$ |
| Monte-Carlo simulations | $10^6$ iterations |

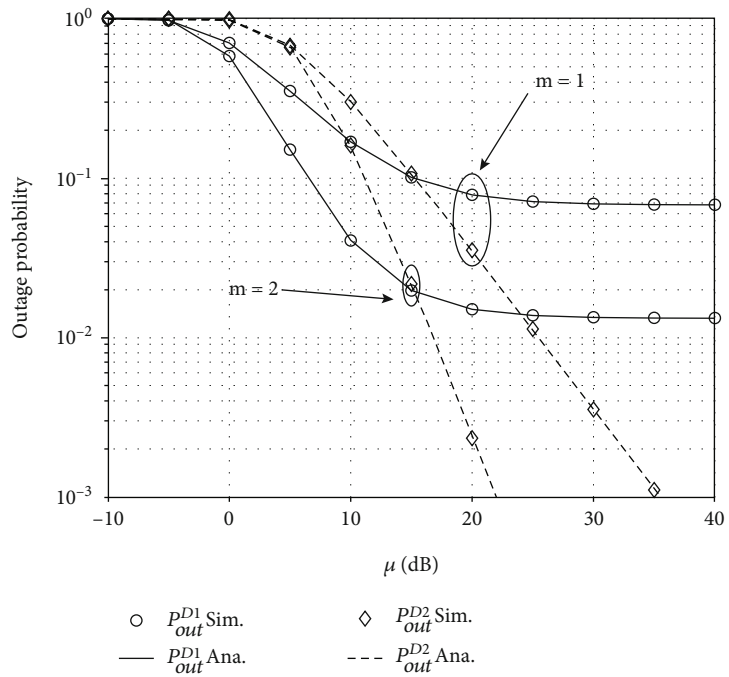


Figure 2: Outage performance vs $\mu$ (dB) varying $m$ with $\eta_t^2 = \eta_r^2 = 0.01$.

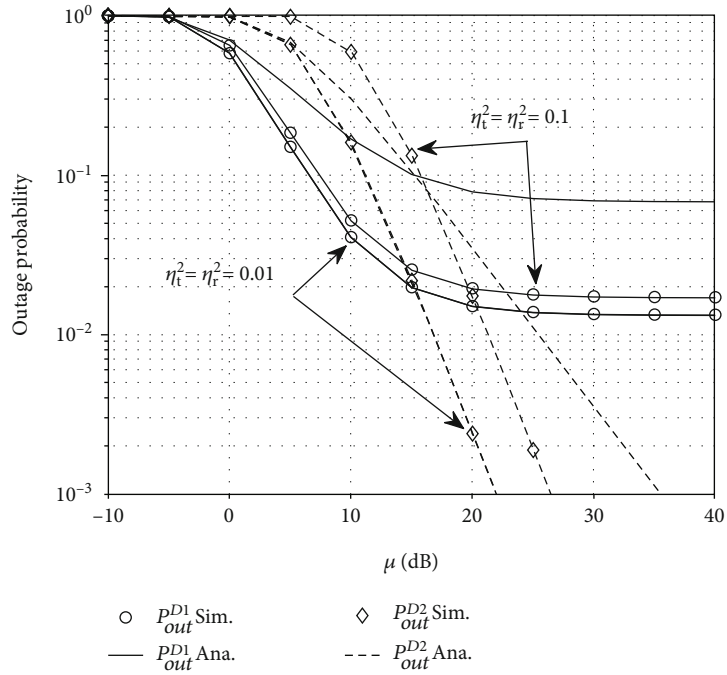


Figure 3: Outage performance vs $\mu$ (dB) varying $\eta_t^2 = \eta_r^2$ with $m = 2$.

## 6. Numerical Results

In this section, we want to illustrate system performance via simulations. In first step, we set $\mu = \mu_S = \mu_R$, and the simulation parameters can be shown in Table 2.

Figure 2 depicts the outage probability of two users versus the transmit SNR at source with two values of fading channel, $m = 1$ and $m = 2$. The exact outage probability curves match with Monte-Carlo simulation. Fortunately, this result confirms our correctness in term of computation of outage probability. We can see the performance gap of two users for the NOMA system over Nakagami-$m$ fading. It can be explained that different signal decoding, number of hops for transmission, and different power allocation factors lead to the performance gap among the two users. We can see that the absence of SIC at $D_1$ results in the outage probability approaching an error floor and failing to go lower in moderate to high SNR regions. It can be concluded that the considered system has better outage behavior once channel condition is improved, i.e., coefficients of Nakagami-$m$ fading are enhanced in specific situations.

We can observe the impact of hardware impairment in our proposed FD NOMA system, shown in Figure 3. By considering the two values of $\eta_t^2 = \eta_r^2$, we see that lower levels of hardware impairment lead to improvement in terms of outage performance. It is clear that $\eta_t^2 = \eta_r^2 = 0.01$ is the better case in terms of outage performance. However, $D_1$ still approaches an error floor in moderate to high SNR regions. It means that such system will work well if we improve signal at the base station. Further, by limiting impact of hardware impairment, such system retains its quality of transmission at downlink.

Figure 4 compares the system associated with FD and HD scenarios. The OP performance of $D_1$ versus transmit SNR is studied while varying values of SNR. The HD case is proven with more benefits in term of OP compared FD-NOMA system. The HD-NOMA system could be better outage compared FD-NOMA system at high SNR region. However, FD-NOMA system exhibits more spectrum efficiency as aforementioned.

In Figure 5, two users are affected by power allocation factors since the corresponding SINRs depend mostly on such allocation factors. Interestingly, the fairness among those users can be changed by such factors. To reduce the overhead in transmission, such factors are hold as fixed values to satisfy demands at users at specific situations. The other trends of OP performance can be seen similarly as previous figures.

In Figure 6, we observe the throughput of the system versus transmit SNR while varying $m$ with $\eta_t^2 = \eta_r^2 = 0.01$. From Figure 6, we can observe different throughput curves depending on $T_{\text{out},i}$. The best throughput performance is achieved by $T_{\text{out},2}$ because destination 2 has a direct link to the base station and does not rely on the relay. Furthermore, depending on the value of i, the best throughput performance is achieved with higher values of fading parameter $m$. However, all the performance curves approach a ceiling at moderate to high SNR regions and fail to go higher, indicating that there are limits to the system determined by the fixed rate $v_1$ in (16) and (17) as can also be seen in Figure 7.

In Figure 8, we observe throughput of the system versus transmit SNR while varying $\eta_t^2 = \eta_r^2$ with $m = 2$. Similar to Figure 6, the $T_{\text{out},2}$ obtains the best performance in the

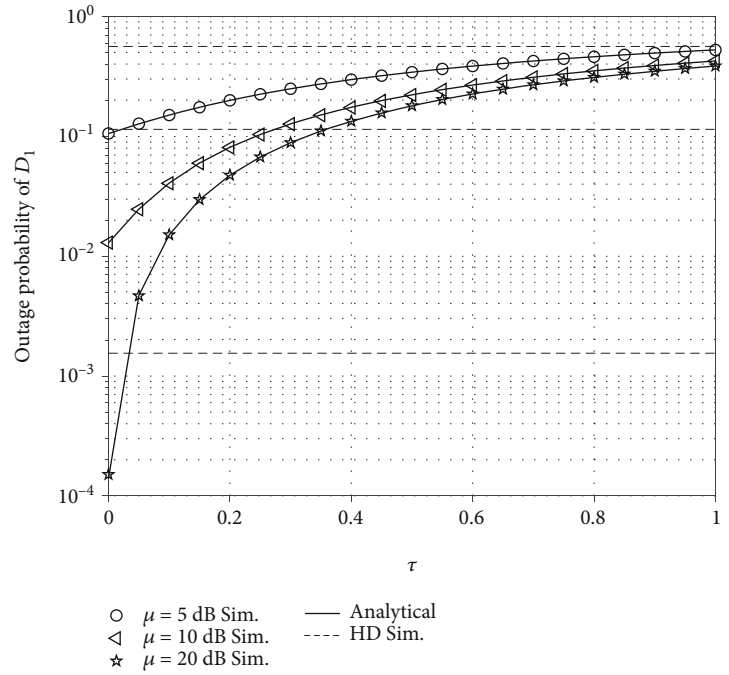


FIGURE 4: Outage performance of $D_1$ vs $\tau$ varying $\mu$(dB) with $m = 2$ and $\eta_t^2 = \eta_r^2 = 0.01$.

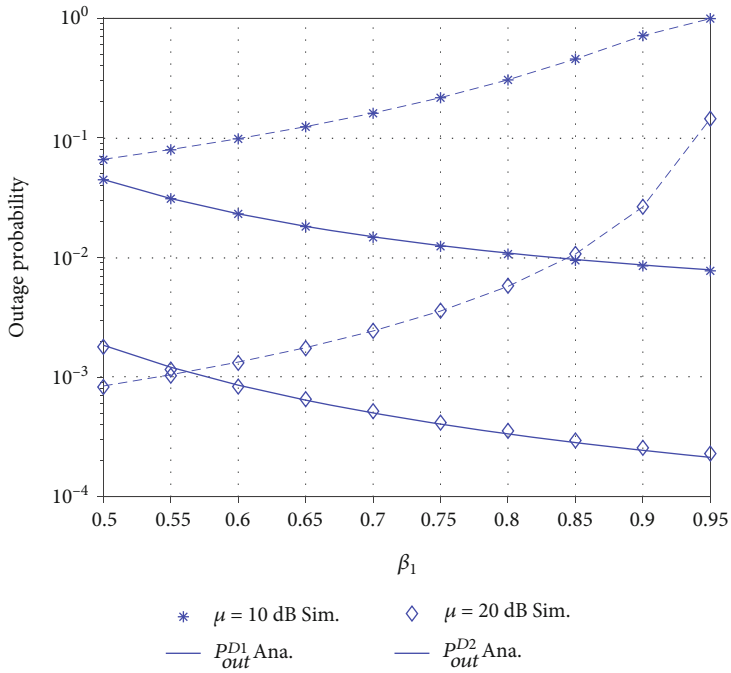


FIGURE 5: Outage performance vs $\beta_1$ varying $\mu$ with $m = 2$ and $\eta_t^2 = \eta_r^2 = 0.01$.

moderate to high SNR region under the considered hardware impairments, though all the performance curves converge at a ceiling at moderate to high SNR regions and fail to go higher despite the level of hardware impairments. It's important to note that at below 0 dB levels, destination 1 outperforms destination 2, this due to the relay, that amplifies and forwards the weak base station transmit signal to destination 2. Here, we can also see the benefits of the relay in the low SNR transmit regions on the cell edge user due to the lack of significant performance variations when $\eta_t^2 = \eta_r^2$ is varied unlike in the case of the centrally located user as can be seen in Figure 8.

The impact of self-interference related to the FD mode at R on throughput performance is studied in Figure 9. In this figure, we observe the impact of increasing $\tau$ on the system throughput performance. There is no significant difference

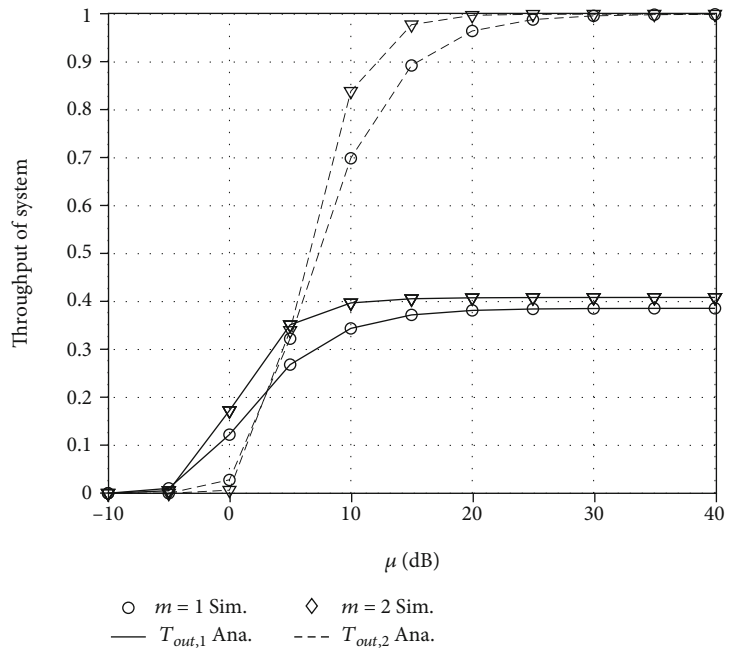


FIGURE 6: Throughput of system vs $\mu$ (dB) varying $m$ with $\eta_t^2 = \eta_r^2 = 0.01$.

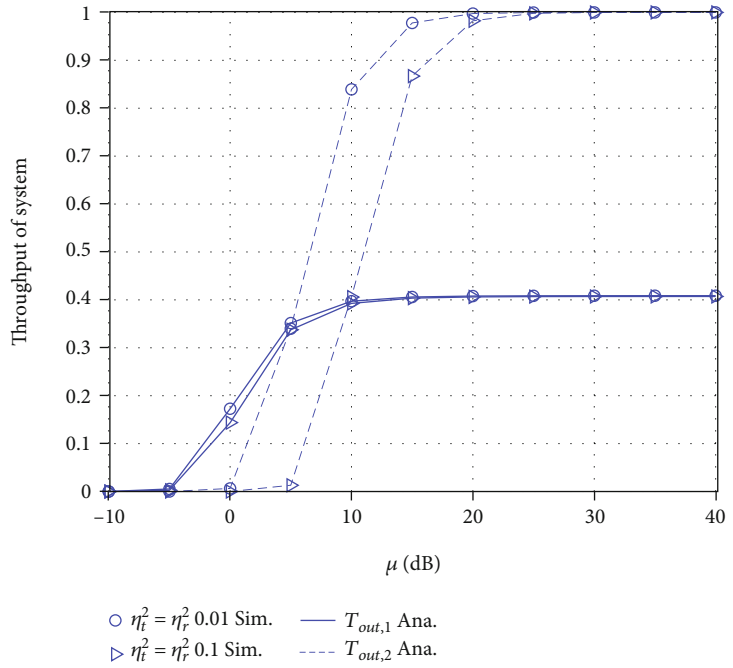


FIGURE 7: Throughput of system vs $\nu_1 = \nu_2$ with $\tau = 0.1$, $\beta_1 = 0.8$, $\beta_2 = 0.2$, and $\mu = 30$dB.

between $\tau = 0.01$ and $\tau = 0.1$ in terms of throughput performance. But, at higher levels of $\tau$, the throughput performance starts to deteriorate. This result is helpful to network designers as they can deploy a suitable FD relay after having thoroughly considered the self-interference values based on the Figure 9.

In Figure 7, we observe that the optimal throughput can be achieved once we have the target rate $\nu_1 = \nu_2$ with $\tau = 0.1$, $\beta_1 = 0.8$, $\beta_2 = 0.2$, and $\mu = 30$dB. At rate $\nu_1 = \nu_2$ greater than 1 and less than about 2.3, the best performance is achieved by the central user. It can be explained that the FD contributes to improve links between the base station and cell-edge user. Figure 7 also depicts the maximum analytical value of each destination user on the $y$ axis as well as the maximum $\nu_1 = \nu_2$ rate on the $x$ axis. Figure 7 demonstrates the limits of throughput when $\nu_1 = \nu_2$ is varied. This result is helpful to network designers intending to deploy this system in practice.

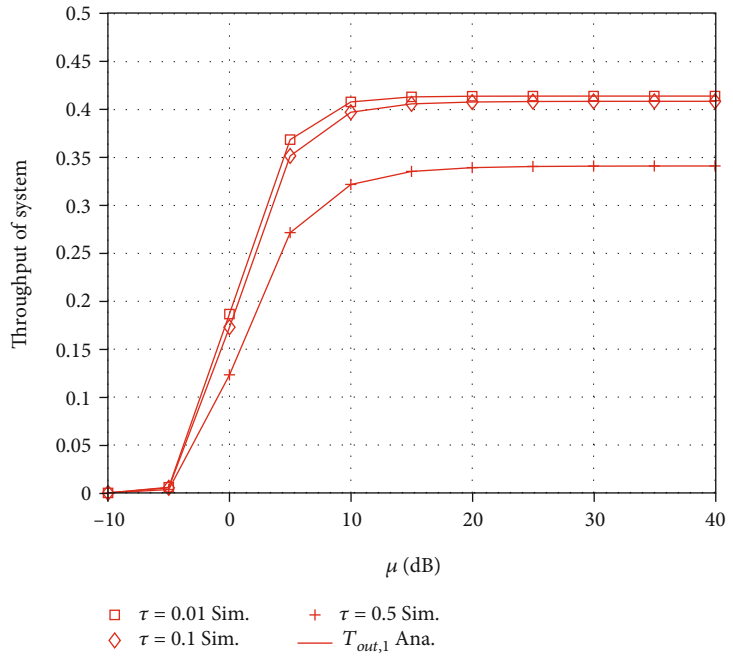


Figure 8: Throughput of system vs $\mu$ (dB) varying $\eta_t^2 = \eta_r^2$ with $m = 2$.

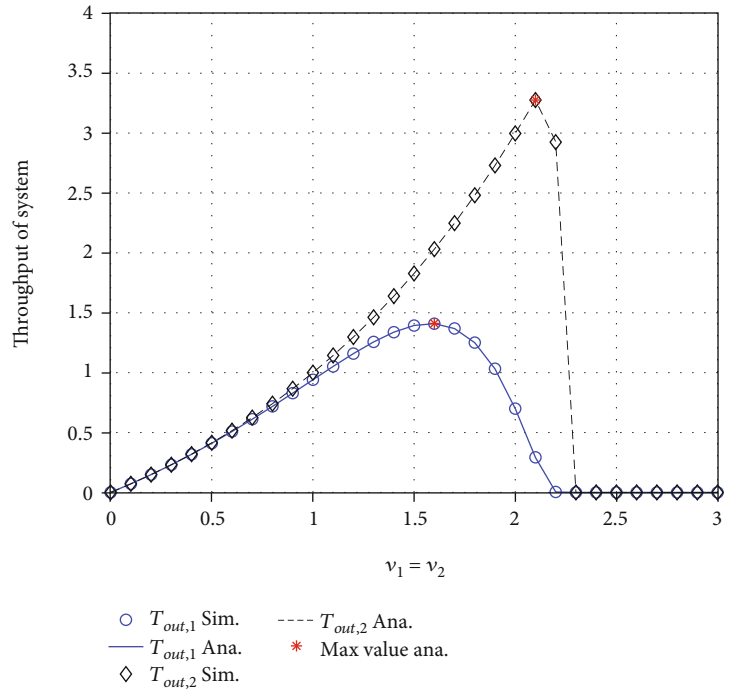


Figure 9: Throughput of system vs $\mu$ (dB) varying $\tau$ with $m = 2$ and $\eta_t^2 = \eta_r^2 = 0.01$.

In all the figures discussed so far, the analytical and simulated results closely match.

## 7. Conclusions

In this paper, we have studied the impact of hardware impairment on the outage performance of FD-NOMA over Nakagami-$m$ fading channels. We characterize two kinds of users depending how far from the base station. The cell-edge user is serviced by the FD-assisted cell-center user. As the main result, new closed-form expressions for the outage probability are derived to evaluate the main factors affecting the system performance. Based on the obtained analytical results, we observed that lower levels of self-interference related to the FD mode and lower levels of hardware impairment can achieve enhancement of the system outage

performance. Finally, the performance gap of these two scenarios was compared in various situations to verify the main impacts on outage probability. In future work, we can deploy multiple antennas at both source and destinations to achieve a larger improvement of outage probability at the destinations.

## Appendix

## A. Proof of Proposition 1

First, (12) can be rewritten as

$$P_{\text{out}}^{D1} = 1 - \underbrace{\Pr\left(\Gamma_{R,x_1} > \vartheta_1\right)}_{\Lambda_1} \underbrace{\Pr\left(\Gamma_{D_1,x_1} > \vartheta_1\right)}_{\Lambda_2}. \tag{A.1}$$

Next, the first term $\Lambda_1$ can be calculated as

$$\begin{aligned}\Lambda_1 &= \Pr\left(|g_{SR}|^2 > \frac{\vartheta_1\left(\mu_R\tau|g_R|^2 + 1\right)}{\mu_S\kappa_R}\right) \\ &= \int_0^\infty f_{|g_R|^2}(z)\int_{\frac{\vartheta_1(\mu_R\tau z+1)}{\mu_S\kappa_R}}^\infty f_{|g_{SR}|^2}(\gamma)d\gamma dz,\end{aligned} \tag{A.2}$$

where $\kappa_R = \beta_1 - \vartheta_1\beta_1 - \vartheta_1(\eta_{R,t}^2 + \eta_{R,r}^2)$. Moreover, we can write (A.2) by

$$\begin{aligned}\Lambda_1 = \sum_{b=0}^{m_{\text{SR}}-1} \frac{e^{-m_{\text{SR}}\vartheta_1/\Omega_{\text{SR}}\mu_S\kappa_R}}{\Gamma(m_R)b!}\left(\frac{m_R}{\Omega_R}\right)^{m_R}\left(\frac{m_{\text{SR}}\vartheta_1}{\Omega_{\text{SR}}\mu_S\kappa_R}\right)^b \int_0^\infty z^{m_R-1} \\ (\mu_R\tau z+1)^b e^{-\left(\frac{m_R}{\Omega_R}+\frac{m_{\text{SR}}\vartheta_1\mu_R\tau}{\Omega_{\text{SR}}\mu_S\kappa_R}\right)z}dz.\end{aligned} \tag{A.3}$$

Based on ([29], 1.111), we can transform $\Lambda_1$ by

$$\begin{aligned}\Lambda_1 = \sum_{b=0}^{m_{\text{SR}}-1}\sum_{c=0}^{b}\binom{b}{c}\frac{(\mu_R\tau)^c e^{-m_{\text{SR}}\vartheta_1/\Omega_{\text{SR}}\mu_S\kappa_R}}{\Gamma(m_R)b!}\left(\frac{m_R}{\Omega_R}\right)^{m_R} \\ \left(\frac{m_{\text{SR}}\vartheta_1}{\Omega_{\text{SR}}\mu_S\kappa_R}\right)^b \int_0^\infty z^{m_R+c-1}e^{-\left(\frac{m_R}{\Omega_R}+\frac{m_{\text{SR}}\vartheta_1\mu_R\tau}{\Omega_{\text{SR}}\mu_S\kappa_R}\right)z}dz.\end{aligned} \tag{A.4}$$

Next, with the help of ([29], 3.351.3) we can obtain $\Lambda_1$ as

$$\begin{aligned}\Lambda_1 = \sum_{b=0}^{m_{\text{SR}}-1}\sum_{c=0}^{b}\binom{b}{c}\frac{\Gamma(m_R+c)(\mu_R\tau)^c e^{-m_{\text{SR}}\vartheta_1/\Omega_{\text{SR}}\mu_S\kappa_R}}{\Gamma(m_R)b!}\left(\frac{m_R}{\Omega_R}\right)^{m_R} \\ \left(\frac{m_{\text{SR}}\vartheta_1}{\Omega_{\text{SR}}\mu_S\kappa_R}\right)^b\left(\frac{m_R}{\Omega_R}+\frac{m_{\text{SR}}\vartheta_1\mu_R\tau}{\Omega_{\text{SR}}\mu_S\kappa_R}\right)^{-m_R-c}.\end{aligned} \tag{A.5}$$

The second term $\Lambda_2$ can be calculated as

$$\Lambda_2 = \Pr\left(\Gamma_{D_1,x_1} > \vartheta_1\right) = \Pr\left(\left|g_{RD_1}\right|^2 > \frac{\vartheta_1}{\mu_R\kappa_{D_1}}\right) = \int_{\frac{\vartheta_1}{\mu_R\kappa_{D_1}}}^\infty f_{|g_{RD_1}|^2}(x)dx, \tag{A.6}$$

where $\kappa_{D_1} = 1 - \vartheta_2(\eta_{D_1,t}^2 + \eta_{D_1,r}^2)$. Similarly, $\Lambda_2$ is obtained as

$$\Lambda_2 = e^{-\frac{m_{RD_1}\vartheta_1}{\Omega_{RD_1}\mu_R\kappa_{D_1}}}\sum_{n=0}^{m_{RD_1}-1}\frac{1}{n!}\left(\frac{m_{RD_1}\vartheta_1}{\Omega_{RD_1}\mu_R\kappa_{D_1}}\right)^n. \tag{A.7}$$

Putting (A.5) and (A.7) into (A.1), (13) is obtained. It completes the proof.

## Data Availability

No data were used to support this study.

## Conflicts of Interest

The authors declare that they have no conflicts of interest.

## Acknowledgments

We are greatly thankful to Van Lang University, Vietnam, for providing the budget for this study.

## References

[1] S. Teodoro, A. Silva, R. Dinis, F. M. Barradas, P. M. Cabral, and A. Gameiro, "Theoretical analysis of nonlinear amplification effects in massive MIMO systems," *IEEE Access*, vol. 7, pp. 172277–172289, 2019.

[2] D. Castanheira, A. Silva, and A. Gameiro, "Retrospective interference alignment for the K -User M x N MIMO Interference Channel," *IEEE Transactions on Wireless Communications*, vol. 15, no. 12, pp. 8368–8379, 2016.

[3] H. Zuo and X. Tao, "Power allocation optimization for uplink non-orthogonal multiple access systems," in *2017 9th International Conference on Wireless Communications and Signal Processing (WCSP)*, pp. 1–5, Nanjing, China, 2017.

[4] Z. Na, J. Lv, F. Jiang, M. Xiong, and N. Zhao, "Joint subcarrier and subsymbol allocation-based simultaneous wireless information and power transfer for multiuser GFDM in IoT," *IEEE Internet of Things Journal*, vol. 6, no. 4, pp. 5999–6006, 2019.

[5] D.-T. Do, M. -S. Van Nguyen, M. Voznak, A. Kwasinski, and J. N. de Souza, "Performance analysis of clustering car-following V2X system with wireless power transfer and massive connections," *IEEE Internet of Things Journal*, 2021.

[6] D.-T. Do, A.-T. Le, Y. Liu, and A. Jamalipour, "User grouping and energy harvesting in UAV-NOMA system with AF/DF relaying," *IEEE Transactions on Vehicular Technology*, vol. 70, no. 11, pp. 11855–11868, 2021.

[7] Z. Song, X. Wang, Y. Liu, and Z. Zhang, "Joint spectrum resource allocation in Noma-based cognitive radio network with SWIPT," *IEEE Access*, vol. 7, pp. 89594–89603, 2019.

[8] D.-T. Do, A. Le, and B. M. Lee, "NOMA in cooperative underlay cognitive radio networks under imperfect SIC," *IEEE Access*, vol. 8, pp. 86180–86195, 2020.

[9] L. Zhang, J. Liu, M. Xiao, G. Wu, Y. Liang, and S. Li, "Performance analysis and optimization in downlink NOMA systems with cooperative full-duplex relaying," *IEEE Journal on Selected Areas in Communications*, vol. 35, no. 10, pp. 2398–2412, 2017.

[10] J. B. Kim and I. H. Lee, "Non-orthogonal multiple access in coordinated direct and relay transmission," *IEEE Communications Letters*, vol. 19, no. 11, pp. 2037–2040, 2015.

[11] C. Zhong and Z. Zhang, "Non-orthogonal multiple access with cooperative full-duplex relaying," *IEEE Communications Letters*, vol. 20, no. 12, pp. 2478–2481, 2016.

[12] R. Tang, J. Cheng, and Z. Cao, "Contract-based incentive mechanism for cooperative NOMA systems," *IEEE Communications Letters*, vol. 23, no. 1, pp. 172–175, 2019.

[13] J. Men, J. Ge, and C. Zhang, "Performance analysis of non-orthogonal multiple access for relaying networks over Nakagami-m fading channels," *IEEE Transactions on Vehicular Technology*, vol. 66, no. 2, pp. 1200–1208, 2017.

[14] S. Lee, D. B. da Costa, Q. T. Vien, T. Q. Duong, and R. T. de Sousa, "Non-orthogonal multiple access schemes with partial relay selection," *IET Communications*, vol. 11, no. 6, pp. 846–854, 2017.

[15] D. Deng, L. Fan, X. Lei, W. Tan, and D. Xie, "Joint user and relay selection for cooperative NOMA networks," *IEEE Access*, vol. 5, pp. 20220–20227, 2017.

[16] Y. Li, Y. Li, X. Chu, Y. Ye, and H. Zhang, "Performance analysis of relay selection in cooperative NOMA networks," *IEEE Communications Letters*, vol. 23, no. 4, pp. 760–763, 2019.

[17] N. Guo, J. Ge, C. Zhang, Q. Bu, and P. Tian, "Non-orthogonal multiple access in full-duplex relaying system with Nakagami-m fading," *IET Communications*, vol. 13, no. 3, pp. 271–280, 2019.

[18] C.-B. Le, D.-T. Do, and M. Voznak, "Exploiting impact of hardware impairments in NOMA: adaptive transmission mode in FD/HD and application in internet-of-things," *Sensors*, vol. 19, no. 6, p. 1293, 2019.

[19] X. Li, J. Li, P. T. Mathiopoulos, D. Zhang, L. Li, and J. Jin, "Joint impact of hardware impairments and imperfect CSI on cooperative SWIPT NOMA multi-relaying systems," in *2018 IEEE/CIC International Conference on Communications in China (ICCC)*, pp. 95–99, 2018.

[20] X. Li, M. Liu, D. Deng, J. Li, C. Deng, and Q. Yu, "Power beacon assisted wireless power cooperative relaying using NOMA with hardware impairments and imperfect CSI," *AEU-International Journal of Electronics and Communications*, vol. 108, pp. 275–286, 2019.

[21] X. Li, Q. Wang, M. Liu et al., "Cooperative wireless-powered NOMA relaying for B5G IoT networks with hardware impairments and channel estimation errors," *IEEE Internet of Things Journal*, vol. 8, no. 7, pp. 5453–5467, 2021.

[22] M. Toka, E. Guven, G. K. Kurt, and O. Kucur, "Performance analyses of MRT/MRC in dual-hop NOMA full-duplex AF relay networks with residual hardware impairments," 2021, https://arxiv.org/abs/2102.08464.

[23] B. C. Nguyen, T. Nguyen-Kieu, T. M. Hoang, P. T. Tran, and M. Vozňák, "Analysis of MRT/MRC diversity techniques to enhance the detection performance for MIMO signals in full-duplex wireless relay networks with transceiver hardware impairment," *Physical Communication*, vol. 42, article 101132, 2020.

[24] X. Li, M. Liu, C. Deng, P. T. Mathiopoulos, Z. Ding, and Y. Liu, "Full-duplex cooperative NOMA relaying systems with I/Q imbalance and imperfect SIC," *IEEE Wireless Communications Letters*, vol. 9, no. 1, pp. 17–20, 2020.

[25] M. S. Van Nguyen, D.-T. Do, Z. D. Zaharis, C. X. Mavromoustakis, G. Mastorakis, and E. Pallis, "Enabling full-duplex in MEC networks using uplink NOMA in presence of hardware impairments," *Wireless Personal Communications*, vol. 120, no. 3, pp. 1945–1973, 2021.

[26] C. Deng, M. Liu, X. Li, and Y. Liu, "Hardware impairments aware full-duplex NOMA networks over Rician fading channels," *IEEE Systems Journal*, vol. 15, no. 2, pp. 2515–2518, 2021.

[27] D.-T. Do and A.-T. Le, "NOMA based cognitive relaying: transceiver hardware impairments, relay selection policies and outage performance comparison," *Computer Communications*, vol. 146, pp. 144–154, 2019.

[28] V. Aswathi and A. V. Babu, "Full/half duplex cooperative NOMA under imperfect successive interference cancellation and channel state estimation errors," *IEEE Access*, vol. 7, pp. 179961–179984, 2019.

[29] I. S. Gradshteyn and I. M. Ryzhik, *Table of Integrals, Series, and Products*, Academic Press, San Diego, CA, 2000.